Propagation of two-dimensional pulses in electromagnetically induced transparency media

Per Arve,* Peter Jänes, and Lars Thylén
Department of Microelectronics and Information Technology, Royal Institute of Technology (KTH), Electrum 229, SE-16440 Kista, Sweden
(Received 29 October 2003; published 14 June 2004)

The propagation in two dimensions of "optical" pulses in electromagnetically induced transparency media is analyzed. Results are presented for coupled Maxwell-Bloch equations with slowly varying envelope approximation, for both adiabatic and nonadiabatic situations. The possibility of changing the direction of the pulse by a switch of control beam direction is investigated in detail.

DOI: 10.1103/PhysRevA.69.063809 PACS number(s): 42.50.Gy, 42.50.Md, 42.25.Bs, 42.79.−e

I. INTRODUCTION

Media that show electromagnetically induced transparency (EIT) can be used to slow or even store light. The EIT is achieved in a so called Λ system, that is atoms or some kind of excitation centers, having a spectrum with three levels arranged as shown in Fig. 1. Level b will normally be the ground state, and a is an excited state with a dipole transition to the ground state, so that there is an appreciable absorption of photons in resonance with the ab transition. A laser beam (control beam) resonant with the ac transition can make the excitation centers transparent for the photons in resonance with ab. The Rabi frequency in the ac transition Ω_c, caused by the control beam, influences the electric (linear) susceptibility of the Λ system [1],

$$\chi(\omega) = -C\frac{\omega-\omega_{ab}+i\gamma_{bc}}{(\omega-\omega_{ab}+i\gamma_{bc})(\omega-\omega_{ab}+i\gamma_{ab})-\Omega_c^2/4}. \quad (1)$$

Here, ω is the electric field angular frequency, ω_{ab} is that of the ab transition, and γ_{ij} is the decay rate of a coherence between the levels i and j. The constant $C=N|\boldsymbol{p}_{ab}|^2/(\epsilon_0\hbar)$ holds the dependence on the density of excitation centers N and the dipole transition element $\boldsymbol{p}_{ab}$. Equation (1) shows that transparency requires γ_{bc} to be small, thus states b and c have to be long lived. If the decay rates are put at zero,

$$\chi(\omega) \approx -\frac{C/2}{\omega-\omega_{ab}+\Omega_c/2}-\frac{C/2}{\omega-\omega_{ab}-\Omega_c/2}, \quad (2)$$

the picture of two dressed states split with $2\Omega_c$ becomes apparent.

The group velocity for a probe pulse with $\omega\approx\omega_{ab}$ will be very small for small Ω_c. The bandwidth for this phenomenon does, on the other hand, also become small. Fleischhauer, Yelin, and Lukin [2,3] considered the possibility of storing light pulses by turning off the control light ($\Omega_c\rightarrow 0$) and then turning it on again to read out the pulse. The situation when the group velocity becomes time dependent due to a time variation of Ω_c was further analyzed by Fleischhauer and Lukin [4,5] in the limit of vanishing or small decoherence rates and adiabatic changes. It has been experimentally shown that the probe pulses can be delayed by the time equal to the duration of the control beam absence [6–8]. Zibrov *et al.* [9] demonstrated the possibility to store a pulse and to revive it in the opposite direction, creating a time reversed version of the original probe pulse. Juzeliunas *et al.* [10] have considered storing light in moving atoms to transport the stored pulse and revive it at the new location.

The motivation for much of these developments has been to create new ways to manipulate well-defined photon states in ways useful for quantum information processing. In the following is presented a theoretical analysis of a method to change the direction of a probe pulse. This may prove useful for quantum information, as well as for manipulating classical optical pulses.

Most of the previous theoretical analysis and experimental work has been confined to one-dimensional situations. A notable exception is the work by Duan *et al.* [11], which addresses quite different aspects than this study.

In order to lift the restriction to one dimension, the Maxwell-Bloch dynamics in two or more dimensions are considered in Sec. II. The different approximations and assumptions are reviewed, and numerical results are presented. In Sec. III are discussed the relations that have to be fulfilled and numerical results of stored pulses revived in the new direction.

II. 2D MAXWELL-BLOCH DYNAMICS

The dynamics of transverse electromagnetic waves are described by the wave equation for the electric field $\boldsymbol{E}$ with the usual polarization $\boldsymbol{P}$ source term

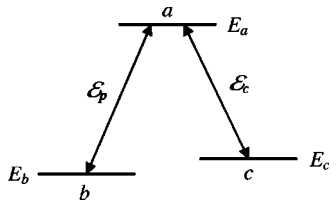

FIG. 1. Level scheme for the levels that produce EIT, with the control field $\mathcal{E}_c$ indicated at the ac transition with which it is resonant. The probe field $\mathcal{E}_p$ is resonant with the transition ab.

*Electronic address: parve@kth.se

$$c^2\nabla^2\boldsymbol{E} - \frac{\partial^2\boldsymbol{E}}{\partial t^2} = \frac{1}{\epsilon_0}\frac{\partial^2\boldsymbol{P}}{\partial t^2}. \tag{3}$$

The medium interacting with the control and probe light is described by the Bloch equations. They give the evolution of the density matrix $\rho_{ij}(\boldsymbol{r},t)$, $i,j=a,b,c$, thus the description entails an averaging. The rationale for this may be twofold. First of all we might aim to only describe the average. Second, medium fluctuations with a much smaller spatial extent than the optical wavelengths do not affect the electromagnetic field much.

In terms of excitation frequencies $\omega_{ij}=(E_i-E_j)/\hbar$, the equations are

$$\frac{\partial}{\partial t}\rho_{ij} = -i\omega_{ij}\rho_{ij} + i\sum_{k=a,b,c}(\boldsymbol{E}\cdot\boldsymbol{p}_{ik}\rho_{kj} - \boldsymbol{E}\cdot\boldsymbol{p}_{kj}\rho_{ik})/\hbar - \gamma_{ij}\rho_{ij} + \delta_{ij}\sum_{k\neq i} b_{ki}\gamma_{kk}\rho_{kk}, \tag{4}$$

where $\boldsymbol{p}_{ij}=e\langle i|\boldsymbol{r}|j\rangle$ are the dipole matrix elements, $\gamma_{ij}(=\gamma_{ji})$ decay rates, and b_{ki} branching ratios. The polarization is calculated from the density matrix elements

$$\boldsymbol{P} = N\sum_{ij}\boldsymbol{p}_{ij}\rho_{ji}, \tag{5}$$

where N is the density of excitation centers (e.g., atoms or quantum dots). This together with Eqs. (3) and (4) constitute the Maxwell-Bloch equations that have been the basis for many investigations of EIT phenomena in one dimension.

We are interested in light pulses much longer than the wavelength, so the electric field is written as

$$\boldsymbol{E}(\boldsymbol{r},t) = \sum_{\alpha}\frac{1}{2}[\boldsymbol{\mathcal{E}}_\alpha(\boldsymbol{r},t)\exp(i\mathbf{k}_\alpha\cdot\boldsymbol{r} - i\omega_\alpha t) + \text{c.c}]. \tag{6}$$

We will only consider situations with one control beam $\alpha=c$ and one beam of probe pulses $\alpha=p$, at any instance of time.

Inserting the expression (6) into Eq. (4) gives a system of equations that is valid for a great variety of fields (6). However, the present discussion will be limited to the following. The control field is in resonance with the *ac* transition, $\omega_c=\omega_{ac}$. Correspondingly, the probe pulses are in resonance with the *ab* transition. The initial amplitudes are such that the Rabi frequencies, Ω_c and Ω_p, fulfill the conditions for the rotating wave approximation, $\Omega_c \ll \omega_{ca}$ and $\Omega_p \ll \omega_{ab}$. The Rabi frequencies are the moduli of the quantities

$$\tilde{\Omega}_c = \boldsymbol{\mathcal{E}}_c\cdot\boldsymbol{p}_{ac}/\hbar, \tag{7}$$

$$\tilde{\Omega}_p = \boldsymbol{\mathcal{E}}_p\cdot\boldsymbol{p}_{ab}/\hbar. \tag{8}$$

Additionally, it is assumed that both $|\boldsymbol{\mathcal{E}}_c\cdot\boldsymbol{p}_{ab}|$ and $|\boldsymbol{\mathcal{E}}_p\cdot\boldsymbol{p}_{ac}|$ are either zero or $\ll\hbar\omega_{cb}=\hbar(\omega_{ab}-\omega_{ac})$. The rapid phase evolution of the density matrix motivates the use of the following quantities:

$$\hat{\rho}_{ii} = \rho_{ii}, \quad i=a,b,c, \tag{9}$$

$$\hat{\rho}_{ab} = \rho_{ab}\exp(-i\boldsymbol{k}_p\cdot\boldsymbol{r} + i\omega_p t), \tag{10}$$

$$\hat{\rho}_{ac} = \rho_{ac}\exp(-i\boldsymbol{k}_c\cdot\boldsymbol{r} + i\omega_c t), \tag{11}$$

$$\hat{\rho}_{bc} = \rho_{bc}\exp[-i(\boldsymbol{k}_c-\boldsymbol{k}_p)\cdot\boldsymbol{r} + i(\omega_c-\omega_p)t]. \tag{12}$$

The Bloch equations now become

$$\frac{\partial}{\partial t}\hat{\rho}_{aa} = \mathrm{Im}\{\tilde{\Omega}_p^*\hat{\rho}_{ab} + \tilde{\Omega}_c^*\hat{\rho}_{ac}\} - \gamma_{aa}\hat{\rho}_{aa}, \tag{13}$$

$$\frac{\partial}{\partial t}\hat{\rho}_{bb} = -\mathrm{Im}\{\tilde{\Omega}_p^*\hat{\rho}_{ab}\} + b_{ab}\gamma_{aa}\hat{\rho}_{aa} + \gamma_{cc}\hat{\rho}_{cc}, \tag{14}$$

$$\frac{\partial}{\partial t}\hat{\rho}_{cc} = -\mathrm{Im}\{\tilde{\Omega}_c^*\hat{\rho}_{ac}\} - \gamma_{cc}\hat{\rho}_{cc} + b_{ac}\gamma_{aa}\hat{\rho}_{aa}, \tag{15}$$

$$\frac{\partial}{\partial t}\hat{\rho}_{ab} = -\frac{i}{2}[\tilde{\Omega}_p(\hat{\rho}_{aa}-\hat{\rho}_{bb}) - \tilde{\Omega}_c\hat{\rho}_{bc}^*] - \gamma_{ab}\hat{\rho}_{ab}, \tag{16}$$

$$\frac{\partial}{\partial t}\hat{\rho}_{ac} = -\frac{i}{2}[\tilde{\Omega}_c(\hat{\rho}_{aa}-\hat{\rho}_{cc}) - \tilde{\Omega}_p\hat{\rho}_{bc}] - \gamma_{ac}\hat{\rho}_{ac}, \tag{17}$$

$$\frac{\partial}{\partial t}\hat{\rho}_{bc} = -\frac{i}{2}[\tilde{\Omega}_c\hat{\rho}_{ab}^* - \tilde{\Omega}_p^*\hat{\rho}_{ac}] - \gamma_{bc}\hat{\rho}_{bc}. \tag{18}$$

Solving Eqs. (13)–(18) for slowly varying Rabi frequencies shows that the elements of $\hat{\rho}$ vary slowly in time.

The time dependence of the polarization $\boldsymbol{P}$ is dominated by frequencies near $\pm\omega_{ab}$ and $\pm\omega_{ac}$, while $\pm\omega_{cb}$ is suppressed as $\boldsymbol{p}_{cb}$ must be small. In view of the previous assumption about the difference of the two frequencies $\omega_{ab}(=\omega_p)$ and $\omega_{ac}(=\omega_c)$ or orthogonality between the dipole matrix elements $\boldsymbol{p}_{ba}\cdot\boldsymbol{p}_{ac}=0$ it may be possible to separate Eq. (3) into different equations. As only the part that interacts with matter is of interest it can be assumed that the electric field directions $\boldsymbol{\mathcal{E}}_{c,p}$ are parallel with the respective dipole moments $\boldsymbol{p}_{ac,ab}$. The vector nature of the equations may then be ignored, hence

$$\left[c^2\nabla^2 - \frac{\partial^2}{\partial t^2}\right]\frac{1}{2}\mathcal{E}_c(\boldsymbol{r},t)\exp(i\boldsymbol{k}_c\cdot\boldsymbol{r} - i\omega_c t) = \frac{Np_{ca}}{\epsilon_0}\frac{\partial^2}{\partial t^2}\rho_{ac}, \tag{19}$$

$$\left[c^2\nabla^2 - \frac{\partial^2}{\partial t^2}\right]\frac{1}{2}\mathcal{E}_p(\boldsymbol{r},t)\exp(i\boldsymbol{k}_p\cdot\boldsymbol{r} - i\omega_p t) = \frac{Np_{ba}}{\epsilon_0}\frac{\partial^2}{\partial t^2}\rho_{ab}. \tag{20}$$

A. Slowly varying envelope approximation

In the previous section, the Bloch equations were simplified assuming that the frequency content of the field amplitudes $\mathcal{E}_{c,p}$ were small. This implies that the field amplitudes correspond to slowly varying envelopes. Thus one may assume that the second order derivatives of the amplitudes $\mathcal{E}_{c,p}$ are negligible compared to the first derivatives on the left-

hand side of Eqs. (19) and (20). On the right-hand sides only the leading term will be kept, to give

$$c\hat{\boldsymbol{k}}_c \cdot \boldsymbol{\nabla}\,\mathcal{E}_c + \frac{\partial \mathcal{E}_c}{\partial t} = i\frac{\omega_c N p_{ca}}{\epsilon_0}\hat{\rho}_{ac}, \tag{21}$$

$$c\hat{\boldsymbol{k}}_p \cdot \boldsymbol{\nabla}\,\mathcal{E}_p + \frac{\partial \mathcal{E}_p}{\partial t} = i\frac{\omega_p N p_{ba}}{\epsilon_0}\hat{\rho}_{ab}. \tag{22}$$

It has been used that $\omega_{c,p}/c = k_{c,p}$, which is the length of $\boldsymbol{k}_{c,p}$, and $\hat{\boldsymbol{k}}_{c,p} = \boldsymbol{k}_{c,p}/k_{c,p}$. The left-hand sides correspond to a wave moving with the velocity c in the direction of $\boldsymbol{k}_{c,p}$. Without the right-hand sides, wave packets will move without changing shape. The approximation gives rise to a propagation of the electromagnetic fields, which is essentially one-dimensional in its character. Hence beam expansion, contraction, or diffraction are neglected. This is reasonable if, as is assumed, the wave vectors $\boldsymbol{k}_{c,p}$ are much larger than those for which the spatial Fourier transform of $\mathcal{E}_{c,p}$ is important. The variation of the wave vector in a direction perpendicular to $\hat{\boldsymbol{k}}_{c,p}$, $\Delta k_\perp$, creates the variation of the propagation direction which is the origin of diffraction. This variation can be neglected if the relative wave vector variation $\Delta k_\perp / k_{c,p} \ll D/L$. Here, D is the spatial extent of important pulse features in a direction perpendicular to $\hat{\boldsymbol{k}}_{c,p}$ and L is the length of propagation. The value of $\Delta k_\perp$ may be taken as $2\pi/D$ which gives the standard rule $L \ll D^2/\lambda$.

B. Adiabatic approximation

Adiabatic approximations have been discussed in [4,12]. The present discussion follows the latter in that Ω_c is assumed to be large, in particular $\gg \Omega_p$. It is also so large that the influence of the decay rates γ_{ij} may be ignored. Together with adiabaticity, i.e., $d\hat{\rho}_{ij}/dt \ll \Omega_c$, this leads to

$$\hat{\rho}^*_{bc} \approx -\frac{\tilde{\Omega}_p}{\tilde{\Omega}_c}, \tag{23}$$

$$\hat{\rho}_{ab} \approx \frac{2i}{\tilde{\Omega}^*_c}\frac{\partial}{\partial t}\frac{\tilde{\Omega}_p}{\tilde{\Omega}_c}, \tag{24}$$

$$\hat{\rho}_{ac} \approx 0. \tag{25}$$

Put into Eqs. (21) and (22) this gives

$$c\hat{\boldsymbol{k}}_c \cdot \boldsymbol{\nabla}\,\mathcal{E}_c + \frac{\partial \mathcal{E}_c}{\partial t} = 0, \tag{26}$$

$$c\hat{\boldsymbol{k}}_p \cdot \boldsymbol{\nabla}\,\mathcal{E}_p + \frac{\partial \mathcal{E}_p}{\partial t} = -\frac{2\omega_p C}{\tilde{\Omega}^*_c}\frac{\partial}{\partial t}\frac{\mathcal{E}_p}{\tilde{\Omega}_c}. \tag{27}$$

For an $\tilde{\Omega}_c$ constant in time, this gives that $\boldsymbol{\mathcal{E}}_p$ moves with the group velocity,

$$v_g = c\frac{\Omega_c^2}{\Omega_c^2 + 2\omega_p C}. \tag{28}$$

That the right-hand side of Eq. (27) is proportional to $\partial\mathcal{E}_p/\partial t$, corresponds to that the electric susceptibility $\chi(\omega)$ is proportional to $\omega - \omega_{ab}$. The group velocity (28) agrees exactly with that calculated from Eq. (2) at $\omega = \omega_{ab}$. The solution to Eq. (27) can be written with $\boldsymbol{r}_\perp$ denoting the part of $\boldsymbol{r}$ perpendicular to $\hat{\boldsymbol{k}}_p$, as

$$\mathcal{E}_p(\boldsymbol{r},t) = f\left(c\hat{\boldsymbol{k}}_p\left[\int_{\sigma(\boldsymbol{r}_\perp)}^{\hat{\boldsymbol{k}}_p\cdot\boldsymbol{r}} \frac{d\xi}{v_g(\hat{\boldsymbol{k}}_p\xi + \boldsymbol{r}_\perp)} - t\right] + \boldsymbol{r}_\perp\right). \tag{29}$$

The function $\sigma(\boldsymbol{r}_\perp)$ is chosen so that $\hat{\boldsymbol{k}}_p\cdot\boldsymbol{r} = \sigma(\boldsymbol{r}_\perp)$ defines a suitable surface, e.g., the surface of probe pulse entry. The function f gives the time dependence of $\mathcal{E}_p$ at the points of this surface given by $\boldsymbol{r}_\perp$.

On the other hand, for an $\tilde{\Omega}_c$ that is constant in space the solution to Eq. (27) is

$$\mathcal{E}_p(\boldsymbol{r},t) = \frac{\tilde{\Omega}_c}{\sqrt{\Omega_c^2 + 2\omega_p C}} f\left(\boldsymbol{r} - \hat{\boldsymbol{k}}_p\int_0^t dt' v_g(t')\right). \tag{30}$$

The group velocity v_g is still given by Eq. (28) and the function $f(\boldsymbol{r})$ gives the shape of the probe field. The state of the medium can also be related to this function, by Eqs. (23) and (24),

$$\hat{\rho}^*_{bc} = -\frac{p_{ab}}{\hbar\sqrt{\Omega_c^2 + 2\omega_p C}} f\left(\boldsymbol{r} - \hat{\boldsymbol{k}}_p\int_0^t dt' v_g(t')\right), \tag{31}$$

$$\hat{\rho}_{ab} = -\frac{2ip_{ab}}{\hbar(\Omega_c^2 + 2\omega_p C)^{3/2}}\left[c\tilde{\Omega}_c\hat{\boldsymbol{k}}_p\cdot\boldsymbol{\nabla} f\left(\boldsymbol{r} - \hat{\boldsymbol{k}}_p\int_0^t dt' v_g(t')\right) + \frac{\Omega_c}{\tilde{\Omega}^*_c}\frac{\partial\Omega_c}{\partial t} f\left(\boldsymbol{r} - \hat{\boldsymbol{k}}_p\int_0^t dt' v_g(t')\right)\right]. \tag{32}$$

In spite of the apparent singularities of $\hat{\rho}_{bc}$ and $\hat{\rho}_{ab}$ as a function of $\tilde{\Omega}_c$ in the expressions (23) and (24), these quantities and $\mathcal{E}_p$ may be well behaved when $\tilde{\Omega}_c \to 0$. Equations (30)–(32) illustrate how the different quantities behave when light is stored.

C. Numerically solved Maxwell-Bloch equations

It is quite feasible to numerically solve the Maxwell-Bloch equations to study short distance propagation in two dimensions. The slowly varying envelope approximation (21) and (22) together with Eqs. (13)–(18), and with real $\tilde{\Omega}_p$, $\tilde{\Omega}_c$, are then sufficient. These equations are solved at a quadratic grid in space by numerical integration of the equations over time. We start with initial values of the density matrix and probe field. The spatial derivatives of the probe field at a grid point are calculated from first order differences between its neighboring points at both sides.

To show how a pulse is stored, Figs. 2 and 3 display the evolution of the control field Rabi frequency Ω_c, the modu-

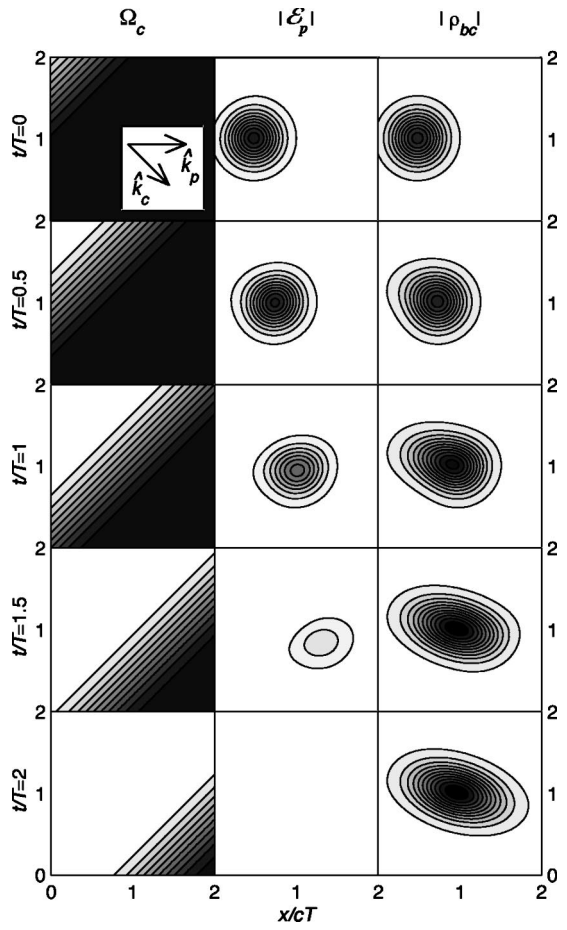

FIG. 2. Adiabatic storing of a light pulse by the EIT mechanism in two dimensions. The results have been obtained without assuming adiabaticity. Dark areas and white areas signify high value and low value, respectively. The left column displays the value of the Rabi frequency $\Omega_c=|\boldsymbol{p}_{ac}\cdot\mathcal{E}_c/\hbar|$, the middle column gives the modulus of the probe pulse $|\mathcal{E}_p|$, and the medium polarization $|\rho_{bc}|$ is shown in the right column. Each row corresponds to an instant of time. The inset in the left part of the top row shows the directions of the two wave vectors. They coincide with the propagation direction of the control field and the initial probe pulse, respectively. At times larger than $2T$ the probe pulse continues to be zero and $|\rho_{bc}|$ stays constant, while the control field moves out of the displayed area.

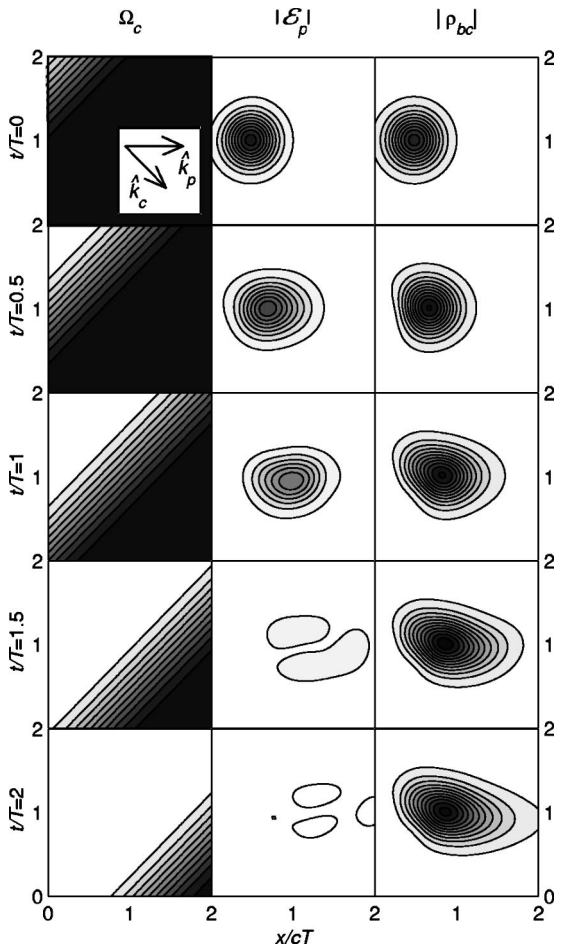

FIG. 3. Nonadiabatic storing of a light pulse by the EIT mechanism in two dimensions. The method to display the results is the same as in Fig. 2. At times larger than $2T$, the remnants of the probe field move in the direction of $\boldsymbol{k}_p$, while $|\rho_{bc}|$ is only affected by the decay given by γ_{bc}. As the control field leaves the region, the probe field moves in an absorbing medium.

lus of the probe pulse envelope $|\mathcal{E}_p|$, and $|\hat{\rho}_{bc}|$. The full width at half maximum time span of the pulse is T which is the time unit and the length unit is cT. The control field and material properties are initially at a value, such that the group velocity $v_g=c/2$. The control field is being turned off, and the trailing edge of the control light appears at the upper left corner at $t=0$ and travels towards the lower right corner, which is the same direction as $\hat{\boldsymbol{k}}_c$. The magnitude of the initial probe field is such that $\Omega_p=1/T$ at the center of the pulse.

In Fig. 2 the initial value of $\tilde{\Omega}_c=500/T$ and the decay parameters are put to zero in order to get an adiabatic situation where the approximations (23) and (24) are valid. The qualitative features expected from Eqs. (30)–(32) are present, though here changes appear locally. Initially, the probe pulse propagates from left to right with velocity $c/2$, and is accompanied by a pulse in $\hat{\rho}_{bc}$ of the same shape and at the same position. The probe field ($\mathcal{E}_p$) decreases when hit by the control beam edge, while the bc coherence $\hat{\rho}_{bc}$ increases and becomes stationary. The part of the probe and the $\hat{\rho}_{bc}$ pulses not yet hit by the edge of the control field, continue forward. This causes an apparent rapid motion of the probe pulse towards the lower left corner. The $\hat{\rho}_{bc}$ pulse, on the other hand, becomes stretched in a direction in between the two propagation directions $\hat{\boldsymbol{k}}_p$ and $\hat{\boldsymbol{k}}_c$, but approximately keeping its magnitude.

In Fig. 3 the initial speed and pulse shape is the same as in Fig. 2, though initially $\tilde{\Omega}_c=10/T$, $\gamma_{aa}=2\gamma_{ab}=2\gamma_{ac}=0.5/T$, $\gamma_{bc}=0.05/T$, and $\gamma_{cc}=0$. The deviations from adiabaticity caused by the rather small values of $\tilde{\Omega}_c$ are seen in the slightly irregular shapes of $\mathcal{E}_p$ and $\hat{\rho}_{bc}$. In particular, the apparently disconnected parts of the probe pulse, seen at $t=1.5T$, are typical for a nonadiabatic process. This is particularly clear at $t=2T$ where it is seen that the probe field remains though the control field has already disappeared. If the trailing edge of the control light is even sharper, this behav-

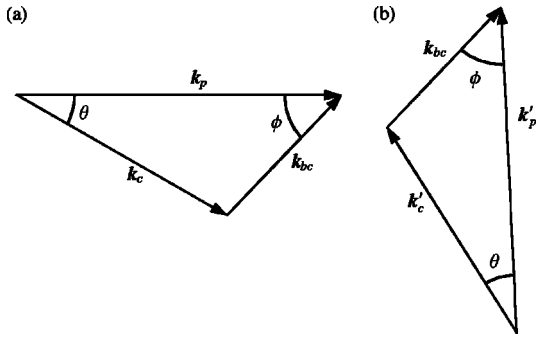

FIG. 4. (a) The relation between the wave vectors for the probe field $\boldsymbol{k}_p$, the control field $\boldsymbol{k}_c$, and the medium excitation $\boldsymbol{k}_{bc}$. (b) The wave vectors of the alternative read out direction.

ior will be even more pronounced. The decay parameters are responsible for decreasing the amplitudes. In particular γ_{bc} governs the decay of $\hat{\rho}_{bc}$ in which the pulse gets stored.

The parameters used in Fig. 3 are quite different from those used by Matsko *et al.* [13]. They found no distortion of the pulse caused by nonadiabatic effects under the circumstance that the pulse bandwidth is much smaller than Ω_c and that the initial group velocity is much smaller than c. The parameters that have been used to produce Fig. 3 violates both those conditions. Thus the distortions of the stored ρ_{bc} and the lingering electromagnetic field at $t=2T$ are not contradicting their findings.

On a technical note, the calculation is simplified by assuming that $\tilde{\Omega}_c$, $\tilde{\Omega}_p$ are initially real, while $\hat{\rho}_{ab}$ and $\hat{\rho}_{ac}$ are imaginary. Then these quantities will continue to be real and imaginary, respectively. Note that before the probe pulse arrives, normally $\hat{\rho}_{bb}=1$ and the other elements are zero. Thus these conditions are satisfied. Additionally, we have simplified the calculation by ignoring $\hat{\rho}_{ac}$ in Eq. (21). This is motivated by that it is small, e.g., compared to ρ_{ab}. Then, assuming that $\boldsymbol{p}_{ab}$ and $\boldsymbol{p}_{ac}$ have similar magnitudes, this source term is insignificant in comparison to the field $\mathcal{E}_c$. At the $x=0$ boundary through which the probe pulse arrives, the x derivative is calculated using the initial Gaussian pulse translated with the group velocity given by $\tilde{\Omega}_c(x=0,t)$. At the other boundaries, the gradient is calculated by smooth continuation.

III. CHANGING THE DIRECTION OF PROPAGATION

The possibility of having an angle between control and probe beams opens up for the possibility of reviving a stored pulse with a differently oriented control beam. Switching its direction by 180° has already been utilized to reverse the probe pulse [9].

In Figs. 2 and 3 is shown the result for a control beam and probe beam that meet at an angle. The quantity $\hat{\rho}_{bc}$ varies smoothly in space and time. From Eq. (12), it is seen that the phase of ρ_{bc} is rapidly changing in time. The spatial variation of the phase is given by the wave vector $\boldsymbol{k}_{bc}=\boldsymbol{k}_p-\boldsymbol{k}_c$, as illustrated in Fig. 4(a). In particular, the stored pulse will have this varying phase. The spatial phase variation shows that there is a linear momentum, frozen into the medium.

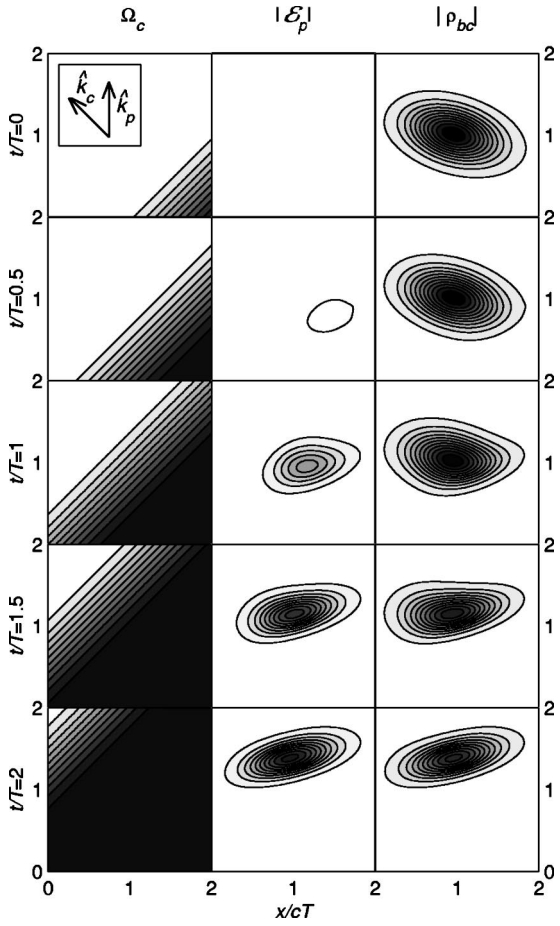

FIG. 5. Adiabatic read out process displayed in the same way as in Fig. 2. At the initial time $t=0$ the medium is in the state from the adiabatic storing one step later than the last shown in Fig. 2, that is, at $t=2.5T$. After the sequence shown $\mathcal{E}_p$ and $\hat{\rho}_{bc}$ move together in the direction of $\boldsymbol{k}_p$ with the velocity $v_g=c/2$.

This is possible as it is assumed that the excitation centers only interact with the electric fields and not directly with each other. Thus, without electric fields, spatial phase differences do not influence the energy and the group velocity of the excitation is zero.

A. Vector relations

As already noted in Ref. [9], the spatial phase variation of the medium excitation ρ_{bc} that remembers the stored probe pulse is important for the read out of the pulse. This phase factor multiplied by the phase factor that comes with a revived control field produces the phase of the probe field source, ρ_{ab}, see Eqs. (22), (10), and (12).

Using that the new control field is still on resonance $\omega_c=\omega_{ac}$, then the frequency of the new probe pulse will also be on resonance $\omega_p=\omega_{ab}$. The condition that the probe field phase variations in time and space are to be correct for a propagating field gives that the new control field wave vector $\boldsymbol{k}'_c$ has to be such that $|\boldsymbol{k}'_c+\boldsymbol{k}_{bc}|=k_p$. In two dimensions only two possibilities exist, shown in Figs. 4(a) and 4(b).

The direction change of the probe beam is 2ϕ, see Figs. 4(a) and 4(b). As the length of the vectors $\boldsymbol{k}_p$ and $\boldsymbol{k}_c$ are fixed,

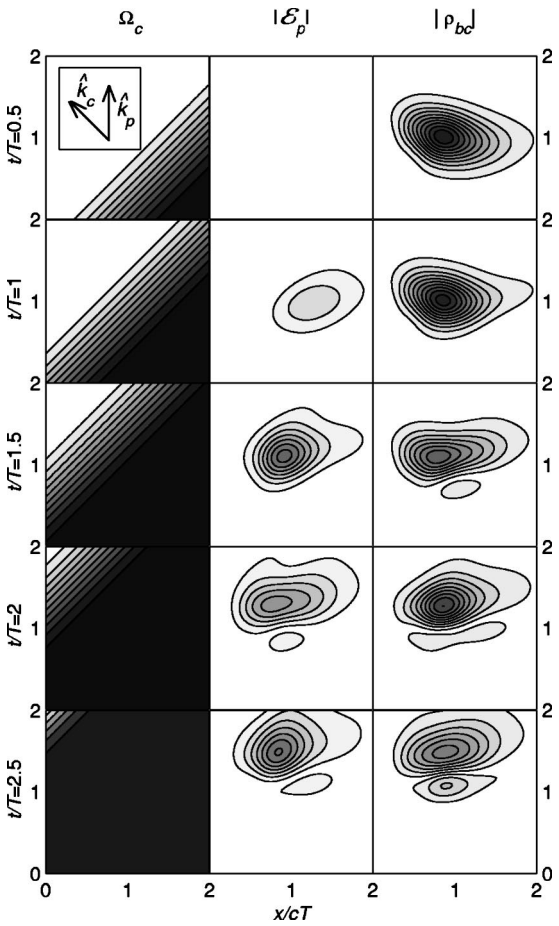

FIG. 6. Nonadiabatic read out process displayed in the same way as in Fig. 2. At the initial time $t=0$ ρ_{bc} is taken from the nonadiabatic storing process (Fig. 3) at $t=2.5T$, while $\mathcal{E}_p$ is put to zero.

the angle ϕ may be viewed as a function of the angle θ. The maximal value of ϕ then arises when there is a right angle between $\boldsymbol{k}_{bc}$ and $\boldsymbol{k}_c$. This happens when cos $\theta=k_c/k_p$ and the maximum value of ϕ is

$$\phi_{\max} = \arcsin(k_c/k_p). \tag{33}$$

For $k_c=k_p$, Eq. (33) gives $\phi_{\max}=\pi/2$, which corresponds to $\boldsymbol{k}_p=\boldsymbol{k}_c$ and $\boldsymbol{k}_{bc}=0$. Thus there is no spatial phase variation, and the revived probe will go in the direction of $\boldsymbol{k}_c'$. As the frequencies of the two fields are the same, their polarizations must be orthogonal in order to distinguish the two beams. When the directions of the beams have changed at least one of the polarizations must also change. This may affect the strength of the revived probe pulse, as the active substates of *b* and *c* (Fig. 1) depend on the polarization of the beams. In Ref. [9] circularly polarized light was used and the direction of the probe pulse was reversed. In this case the polarization vectors were unchanged, but as the propagation direction was reversed, the $\sigma_\pm$ character switched. This enabled a complete time reversal.

It is possible to use linearly polarized light to store and read light pulses [14]. If the frequencies are different enough to distinguish control and probe beam, then both beams can

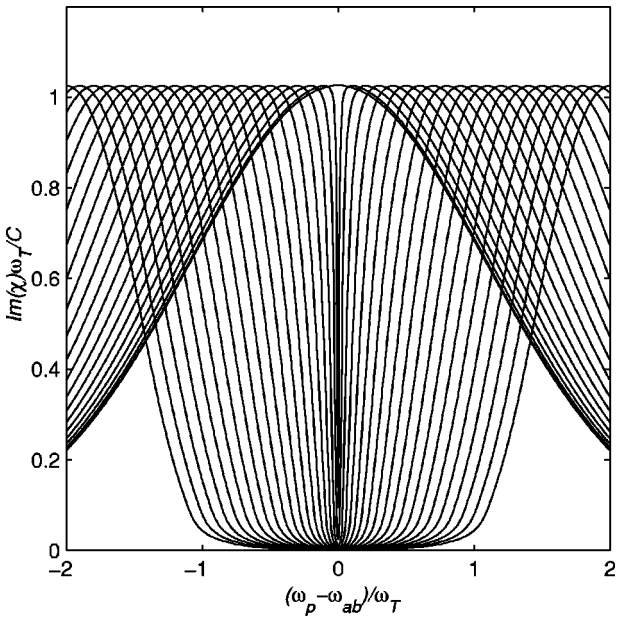

FIG. 7. The imaginary part of the susceptibility for a Maxwell-Boltzmann gas of atoms. The two wave vectors are identical, $\boldsymbol{k}_p=\boldsymbol{k}_c$. The different curves correspond to $\Omega_c/\omega_T=0,0.2,\ldots,4$, $\gamma_{ab}/\omega_T=0.25$, $\gamma_{cb}/\omega_T=0.001$, and $\omega_c+\omega_{cb}=\omega_{ab}$. The quantity $\omega_T=(k_BT/m)^{1/2}k_p$ gives the thermal Doppler broadening of the angular frequency ω_{ab}. The bell-shaped curve is for $\Omega_c=0$, the curve with a narrow dip is for $\Omega_c=0.2\omega_T$, and the larger Ω_c the wider and lower minima.

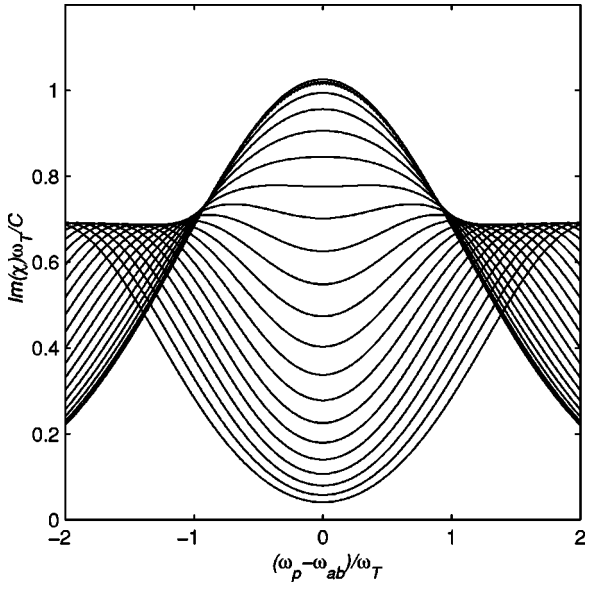

FIG. 8. The imaginary part of the susceptibility for a Maxwell-Boltzmann gas of atoms. The two wave vectors are the same as in the storing process, Figs. 2 and 3. All other parameters are the same as in Fig. 7. The bell-shaped curve ($\Omega_c=0$) is therefore the same. The curves for finite Ω_c are different and there is no dip for $\Omega_c/\omega_T<1$.

be linearly polarized perpendicular to the plane of the wave vectors. The new directions shown in Fig. 4(b) will be available without loss of pulse amplitude due to polarization mismatch.

B. The read out process

For the pulses stored in the processes shown in Fig. 2 and 3, the angle θ was $\pi/4$. If $k_p/k_c=\sqrt{2}$ this corresponds to $\phi=\phi_{\max}=\pi/4$. The deflection of the probe beam is then $\pi/2$ and $\boldsymbol{k}_c'=-\boldsymbol{k}_c$. Such a read out process has been numerically calculated based on the stored pulses. In Figs. 5 and 6 is displayed the read out of the pulse stored as shown in Figs. 2 and 3, respectively. The material parameters are the same as previous. The control field starts at zero and is turned on, creating a front that moves from the lower right corner to the upper left. The control field is ramped up to the same value as when the storing started so that $v_g=c/2$ at the end of the read out sequence.

Common for both the adiabatic and nonadiabatic read out processes is that the probe electromagnetic field is revived by the control field. The new probe pulses end up with a velocity $c/2$ in the direction of $\boldsymbol{k}_p'$ (upwards), though in the nonadiabatic case this is only true for the main part of the pulse.

In the adiabatic process, Fig. 5, it is noticeable how well-formed the probe pulse and $\hat{\rho}_{bc}$ are at all times. However, the pulse does not retain the same shape as the original pulse in Fig. 2, but the read out pulse has an elliptic shape. The elongated direction is almost perpendicular to the new direction of propagation. This is in contrast to if the read control field comes in the same direction as during writing. Then the revived probe pulse will retain its original shape as well as the direction.

For the weaker control field the somewhat chaotic motion gives rise to a slightly deformed probe pulse, see Fig. 6. The finer detail of the pulse shape may be lost, but for purposes similar to the amplitude modulated digital fiber-optic information techniques of today, enough information is still retained. Two salient features of the exciting pulse are the appearance of a satellite trailing the main part and the oscillation of the $|\mathcal{E}_p|$ and $|\rho_{bc}|$. Both are consequences of the lack of adiabaticity.

IV. CONCLUDING REMARKS

The present analysis is general and not gauged towards any specific physical system. So far, except for [8], the storing of pulses has been realized in gases [6,7,9]. A few problems related to realizing the scenarios analyzed in this paper are discussed below.

First, for the nonzero angle between the two beams, the doppler shifts caused by the thermal motion make the transparency window disappear for small Ω_c, see Figs. 7 and 8. This can be arrived at by generalizing Eq. (1) to $\omega_c-\omega_{ac}\neq 0$ and doppler shifting the frequencies $\omega_\alpha\rightarrow\omega_\alpha-\boldsymbol{v}\cdot\boldsymbol{k}_\alpha$ [15], due to the atoms moving with velocity $\boldsymbol{v}$ and integrating over the Maxwell-Boltzmann velocity distribution $P(\boldsymbol{v})$ in the plane of $\boldsymbol{k}_p$ and $\boldsymbol{k}_c$,

$$\chi(\omega_p)=\int\int d^2v P(\boldsymbol{v})\frac{-C[\omega_p-\omega_c-\omega_{bc}-\boldsymbol{v}\cdot(\boldsymbol{k}_p-\boldsymbol{k}_c)+i\gamma_{bc}]}{[\omega_p-\omega_c-\omega_{bc}-\boldsymbol{v}\cdot(\boldsymbol{k}_p-\boldsymbol{k}_c)+i\gamma_{bc}](\omega_p-\omega_{ab}-\boldsymbol{v}\cdot\boldsymbol{k}_p+i\gamma_{ab})-\Omega_c^2/4}. \tag{34}$$

For a class of atoms with velocity $\boldsymbol{v}$ the transparency maximum is achieved when

$$\omega_p-\omega_c-\omega_{bc}-\boldsymbol{v}\cdot(\boldsymbol{k}_p-\boldsymbol{k}_c)=0, \tag{35}$$

if γ_{bc} is neglected. The frequency ω_p for which Eq. (35) is fulfilled will vary with the velocity. Only by making $\Omega_c\gg v_T k_{bc}$ will the transparency windows overlap for the different velocity classes within the thermal distribution. Here v_T is the thermal velocity of the atoms. Large Ω_c means large v_g and possibly incoherence in the control beam inducing a reduction of ρ_{bc}. However, a 90° angle between the probe and control beams was used [16] when achieving $v_g=17$ m/s.

Second, the thermal motion may wash out a stored spatial variation of ρ_{bc}, in particular, a rapid phase variation caused by a large $\boldsymbol{k}_{bc}$. In a rarefied gas the atoms structures of ρ_{bc} of length L disolve at a rate v_T/L. The rate for the phase variation is then $v_T k_{bc}/2\pi$. For visible wavelengths and $k_{bc}\sim k_p$ then the rate is 10^9 s^{-1}. In rubidium and similar systems one may have $v_T(k_p-k_c)\sim 10$ kHz. The addition of a buffer gas will decrease this considerably as it slows down the diffusion.

One may hope that a large set of physical systems can show EIT. The realization of slow light in Pr doped Y_2SiO_5 [8] gives hope for this in other solids, e.g., semiconductor systems [17–19]. The mechanism discussed in this paper may prove useful for several applications. Other types of technological devices based on EIT have previously been suggested [20,21].

ACKNOWLEDGMENTS

Valuable discussions with Björn Hessmo, Jonas Tidström, and Eilert Berglind at the Royal Institute of Technology are acknowledged.

[1] M. O. Scully and M. S. Zubairy, *Quantum Optics* (Cambridge University Press, Cambridge, England, 1997).
[2] M. D. Lukin, S. F. Yelin, and M. Fleischhauer, Phys. Rev. Lett. **84**, 4232 (2000).
[3] M. Fleischhauer, S. F. Yelin, and M. D. Lukin, Opt. Commun. **179**, 395 (2000).
[4] M. Fleischhauer and M. D. Lukin, Phys. Rev. Lett. **84**, 5094 (2000).
[5] M. Fleischhauer and M. D. Lukin, Phys. Rev. A **65**, 022314 (2002).
[6] C. Liu, Z. Dutton, C. H. Behroozi, and L. V. Hau, Nature (London) **409**, 490 (2001).
[7] D. F. Phillips, A. Fleischhauer, A. Mair, R. L. Walsworth, and M. D. Lukin, Phys. Rev. Lett. **86**, 783 (2001).
[8] A. V. Turukhin, V. S. Sudarshanam, M. S. Shahriar, J. A. Musser, B. S. Ham, and P. R. Hemmer, Phys. Rev. Lett. **88**, 023602 (2002).
[9] A. S. Zibrov, A. B. Matsko, O. Kocharovskaya, Y. V. Rostovtsev, G. R. Welch, and M. O. Scully, Phys. Rev. Lett. **88**, 103601 (2002).
[10] G. Juzeliunas, M. Masalas, and M. Fleischhauer, Phys. Rev. A **67**, 023809 (2003).
[11] L.-M. Duan, J. I. Cirac, and P. Zoller, Phys. Rev. A **66**, 023818 (2002).
[12] M. Fleischhauer and A. S. Manka, Phys. Rev. A **54**, 794 (1996).
[13] A. B. Matsko, Y. V. Rostovtsev, O. Kocharovskaya, A. S. Zibrov, and M. O. Scully, Phys. Rev. A **64**, 043809 (2001).
[14] H. Gao, M. Rosenberry, and H. Batelaan, Phys. Rev. A **67**, 053807 (2003).
[15] O. Kocharovskaya, Y. Rostovtsev, and M. O. Scully, Phys. Rev. Lett. **86**, 628 (2001).
[16] L. V. Hau, S. E. Harris, Z. Dutton, and C. H. Behroozi, Nature (London) **397**, 594 (1999).
[17] C. C. Phillips, E. Paspalakis, G. B. Serapiglia, C. Sirtori, and K. L. Vodopyanov, Physica E (Amsterdam) **7**, 166 (2000).
[18] M. Phillips and H. Wang, Phys. Rev. Lett. **89**, 186401 (2002).
[19] M. Phillips and H. Wang, Opt. Lett. **28**, 831 (2003).
[20] M. Davanço, P. Holmström, D. J. Blumenthal, and L. Thylén, IEEE J. Quantum Electron. **39**, 608 (2003).
[21] P. C. Ku, C. J. Chang-Hasnain, and S. L. Chuang, Electron. Lett. **38**, 1581 (2002).